



Research papers

Improving snowpack chemistry simulations through improved representation of liquid water movement through layered snow and rain-on-snow (ROS) episodes: Application to Svalbard, Norway

Diogo Costa ^{a,b,*}, Andrea Spolaor ^{c,d}, Elena Barbaro ^{c,d}, Juan I. López-Moreno ^e, John W. Pomeroy ^{b,f}

^a MED – Mediterranean Institute for Agriculture, Environment and Development & CHANGE – Global Change and Sustainability Institute, Department of Geosciences, University of Évora, Pólo da Mitra, Ap. 94, 7006-554 Évora, Portugal

^b University of Saskatchewan, Department of Geography and Planning, Saskatoon, Canada

^c Institute of Polar Sciences - National Research Council of Italy (CNR-ISP), Via Torino 155, (I) 30172 Venezia-Mestre (VE), Italy

^d Ca' Foscari University of Venice, Department of Environmental Sciences, Informatics and Statistics, Via Torino 155, 30170 Venice Mestre, Italy

^e Instituto Pirenaico de Ecología, Consejo Superior de Investigaciones Científicas (IPE-CSIC), Campus de Aula Dei, Apartado 13.034, 50.080 Zaragoza, Spain

^f Centre for Hydrology, University of Saskatchewan, Canmore, Canada

ARTICLE INFO

This manuscript was handled by Marco Borga, Editor-in-Chief.

Keywords:

Cryosphere
Snowpack
Chemistry
Transport
Numerical modelling

ABSTRACT

Circumpolar and high-elevation cold regions receive a large portion of their annual precipitation as snowfall, which accumulates in snowpacks that can store many contaminants. The discharge of chemical eluent during snowmelt can alter the chemical composition of local streams and have a detrimental effect on aquatic ecosystems.

Cold regions have been particularly affected by climate change. In the last two decades, the Arctic has been exposed to dramatic atmospheric temperature increases, sea ice decrease, and an increase of air mass transport from lower latitudes bringing warmer and more humid air masses. Instrumental measurements in the Svalbard archipelago, Norway, show that climate warming here is amplified compared to the global average, making its cryospheric environment extremely vulnerable to future climate scenarios.

In this study, the PULSE model for simulation of snowpack solute dynamics was coupled to two snowpack energy balance models, the Cold Regions Hydrological Model and the SNOWPACK model, to help identify critical processes needed to improve the accuracy of snow chemistry predictions. Focus was given to Na^+ to represent sea spray sources, Ca^{2+} to represent terrestrial dust, and SO_4^{2-} to represent various sources including sea salt, biogenic emissions, and long-range atmospheric transport of secondary aerosols. The new coupled models were applied to an experimental site in Svalbard. The hydrological components of each model coupling were validated against snowdepth measurements and the snowpack chemistry components were verified for a selected number of snow ions representative of different sources. Both models were able to predict snowdepths between 1996 and 2018, as well as the stratification of snow chemistry measured during a whole snow accumulation and ablation year. Results show that explicitly representing liquid water movement through layered snow helped improve chemistry predictions. Events such as rain-on-snow (ROS) had a disproportionate effect on the redistribution of ions to deeper snow layers.

1. Introduction

The Arctic is being disproportionately affected by climate change. For example, a mean warming rate of $+1.35\text{ }^\circ\text{C}$ per decade has been observed in the Norwegian archipelago of Svalbard, located in the Arctic Ocean, which is much faster than the global average (Isaksen et al., 2016; Maturilli et al., 2013; Nordli et al., 2014; Spolaor et al., 2023).

Analogous to other regions in the Arctic, Svalbard exhibits mountains, glaciers, tundra vegetation species, and lakes (Beldring et al., 2008). Hydrological processes, such as glacier runoff and permafrost thawing, have been strongly affected by changes in water and energy balances due to a surge in air temperature and precipitation (Nowak and Hodson, 2013). This region, located at the current southern edge of the

* Corresponding author at: MED – Mediterranean Institute for Agriculture, Environment and Development & CHANGE – Global Change and Sustainability Institute, Department of Geosciences, University of Évora, Pólo da Mitra, Ap. 94, 7006-554 Évora, Portugal.

E-mail address: diogo.costa@uevora.pt (D. Costa).

<https://doi.org/10.1016/j.jhydrol.2024.132573>

Received 15 July 2024; Received in revised form 3 December 2024; Accepted 4 December 2024

Available online 31 December 2024

0022-1694/© 2025 The Authors. Published by Elsevier B.V. This is an open access article under the CC BY license (<http://creativecommons.org/licenses/by/4.0/>).

multiyear sea ice in the North Atlantic Ocean, is characterized by a maritime climate with large, rapid temperature variations during winter (Hansen et al., 2014). Mild oceanic air masses from the southwest can bring relatively warm and moist air in winter months, while polar airmass intrusions from the northeast, driven by a high-pressure system over Greenland, result in much colder temperatures (Rinke et al., 2017). In addition to these synoptic fluctuations, intense autumn or winter cyclonic storms associated with anomalous warming events sometimes occur, transporting both heat and moisture from lower latitudes (Rinke et al., 2017) and causing rapid oscillations in its meteorological conditions, from polar to maritime. The aforementioned meteorological conditions also favour long-range atmospheric transport of aerosols to this archipelago, including pollutants from continental sources. Global warming may change contaminant loading and biogeochemical cycling in the Arctic, changing the synoptic conditions (Larose et al., 2013a,b).

During snowmelt, meltwater percolates through the snowpack and transports chemicals at the ice-water-air interface as hydraulic conductivity increases (Bales et al., 1989). Although many knowledge gaps exist in understanding air-ice chemical and physical interactions in liquids, quasi-liquids, and solids in snow (Bartels-Rausch et al., 2014), it has been observed that snow ions are removed from the snowpack through a process of preferential elution (Brimblecombe et al., 1985). It is understood that this process arises from ice crystal metamorphism and low solubility in ice (Cragin et al., 1993), which promotes snow ion exclusion and the reallocation of ions in the snowpack (Brimblecombe et al., 1985). Basins that have a limited ability to neutralize acids can change chemical composition due to snowmelt (Bales et al., 1989), which may cause stressful conditions for aquatic ecosystems (Marsh and Pomeroy, 1999).

Temperature and pressure affect the physical and chemical properties of water that coexist in different phases (water vapour, liquid and ice). The formation of snow crystals requires atmospheric temperatures below 0 °C and the presence of supercooled water. These conditions and the complexity and heterogeneity of contact between water molecules and other chemical molecules and ions make snow hydro-chemical modelling, along with temperature, pressure and spatiotemporal gradients, a challenging task. Seasonal snowpacks typically contain nutrients, soluble inorganic and organic matter, and various other contaminants delivered via wet and dry deposition (Larose et al., 2013a). Snowpacks also often contain trace gases, such as sulfur dioxide (SO₂), carbon dioxide (CO₂), and nitrous oxide (N₂O), as well as aerosols such as pollen, sea salt particles, mineral dust and sulphates (Hodson et al., 2008). The release of chemicals from snowpacks during snowmelt is a complex physicochemical process (Bartels-Rausch et al., 2014) that typically results in an early ionic pulse in snowpack meltwater discharge (Davies et al., 1987; Lilbæk and Pomeroy, 2010; Costa and Pomeroy, 2019; Costa et al., 2020). It has been observed that some controls of this ionic pulse are the snow depth, melt rate and distribution of ions within the snowpack (Marsh and Pomeroy, 1999; Costa et al., 2018; Costa and Pomeroy, 2019).

Climate change is expected to increase the frequency of rain-on-snow (ROS) events by 50% with a temperature rise of up to 2–4 °C (Beniston and Stoffel, 2016; Morán-Tejeda et al., 2016). Such events accelerate the development of preferential flowpaths (PFP) in snowpacks, affecting the snowpack discharge process. In a lab experiment using high-frequency flow and chemistry measurements, (Costa et al., 2020) found that naturally forming PFP released and transported 3.5%, 25%, 20%, and 4% of the total Cl⁻, NO₃⁻, PO₄³⁻, and SO₄²⁻ snow load during the first 1.5% of snowmelt, but ROS helped to dilute the magnitude of this early ionic pulse. Being able to predict how snowpacks store and release contaminants and how they will respond to climate change has become extremely important to anticipate and mitigate the potential adverse effects on aquatic ecosystem (Lapalme et al., 2023). Early advances in this area date back to the (Stein et al., 1986) empirical model for the estimation of snowmelt runoff

concentration peaks from pre-melt average snow concentrations and snow water equivalent (SWE) dynamics, which is a simple approach that has been successfully used in several studies (e.g. Costa et al., 2017). More physically-based approaches have followed (Bales, 1991; Harrington et al., 1996; Hibberd, 1984), which used porous media flow theory. For instance, Harrington et al. (1996) used the 1D vertical advection–dispersion equation to simulate solute transport through melting snowpacks. More recently, Costa et al. (2018, 2020) extended this approach to represent more explicitly the evolution of in-snow solid and liquid solute (multiphase) concentrations during snowmelt.

The objective of the present study is to help further enhance snow chemistry predictions. In particular, we explored the effect of considering a simpler 2-layer model versus a multilayer modelling approach resolving liquid water movement through layered snow. The coupled models were combined with snowpit density and chemistry data collected in Svalbard, which is an Arctic Archipelago located between mainland Norway and the North Pole. It has a polar climate, characterized by long, cold winters, short, cool summers, and persistent snow and ice cover, with seasonal variations in daylight due to its high latitude. The study focused on two main objectives (1) to improve the prediction of spatiotemporal variability in snowpack and meltwater chemistry, and (2) to help determine the effect of rapid temperature variations during winter in Svalbard (Hansen et al., 2014) on the snowpack microstructure and snowpack and snowmelt runoff chemistry.

2. Materials & methods

2.1. Snow chemistry: The original standalone PULSE model

The PULSE model, as described by Costa et al. (2018, 2020), was developed to simulate snowpack solute dynamics and capture runoff ionic pulses. It builds upon the snow chemistry modelling framework introduced by Harrington and Bales (1998). It is a multi-layer, multiphase finite-volume numerical model of the snowpack that includes three interacting water phases: solid (snow grain core), quasi-liquid (snow grain surface), and liquid (refer to Fig. 1). The model aims to simulate the vertical and temporal evolution of snowpack chemistry to predict ionic pulses in meltwater discharge. It incorporates mechanisms of snow ion exclusion and preferential elution, capturing temporal and vertical profile concentration changes during snowmelt, as observed by Davis et al. (1995). Despite knowledge gaps in understanding air-ice chemical and physical interactions in liquids, quasi-liquids, and solids in snow (Bartels-Rausch et al., 2014), it is generally accepted that ion exclusion occurs during snow metamorphism, where some snow grains lose mass while others gain it. Volatile ionic solutes from the grains losing mass accumulate on the surface of adjacent snow grains (Harrington and Bales, 1998) because ions are not easily incorporated into growing crystal lattices, leading to their exclusion and subsequent accumulation on the surfaces of snow grains (Hewitt et al., 1991). The rates of ion exclusion vary based on ion diffusion rates and solubility in ice, influenced by the hydrated radii of the ions and their ability to form hydrogen bonds (Lilbæk and Pomeroy, 2008), resulting in preferential elution.

In PULSE, the mass balance of the solid phase includes the snow grain core (c_{sc} , Eq. (1)) and the snow grain surface (c_{ss} , Eq. (2)).

$$\frac{\partial(\theta_{sc}c_{sc})}{\partial t} = -c_{sc} \cdot \theta_{sc} \cdot q \cdot \frac{\rho_s}{\rho_l} \quad (1)$$

where ρ_s and ρ_l are snow and liquid water densities, θ_{sc} is the volume fraction occupied by the snowpack solid phase, and q is the melt rate.

$$\frac{\partial(\theta_{ss}c_{ss})}{\partial t} = c_{sc} \cdot \theta_{sc} \cdot q \cdot \frac{\rho_s}{\rho_l} - E \cdot \theta_{ss} \quad (2)$$

where θ_{ss} is the volume fraction occupied by the snowpack liquid phase and E is the solute mass exchange between the surface of the snow grain and the mobile (liquid) phase. In the original standalone PULSE

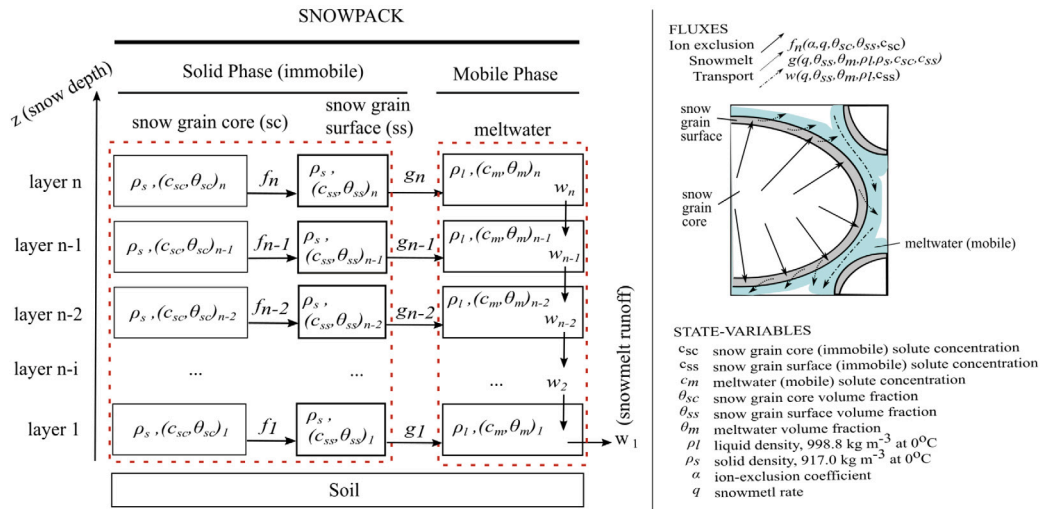


Fig. 1. Conceptual model (right panel) and flowchart of the numerical framework (left panel) used to simulate snowpack solid and liquid phase evolution during melt. (For interpretation of the references to colour in this figure legend, the reader is referred to the web version of this article.)
Source: Adapted from Costa et al. (2018).

model, the snow grain core mass (Eq. (1)) is assumed to decrease via a first-order (exponential) decay process that is also controlled by the melt rate (q). The total mass in the snow grain surface (Eq. (2)) depends on the snow grain core mass that has melted. The exchange of mass between the snow grains surface and the moving liquid mobile water (E) is described as,

$$E = \alpha(c_{ss} - c_m) \quad (3)$$

where c_{ss} and c_m are the concentrations at the surface of the snow grains (ss) and in meltwater (m) and α is a parameter to account for ion exclusion.

While the ion exclusion process is known to vary with the ionic species, field observations indicate additional, not fully understood controls e.g. Johannessen et al. (1976) and Johannessen and Henriksen (1978). Brimblecombe et al. (1985) suggested that these controls may include snowpack inhomogeneity, pre-melt ion concentration, and the history of melting and refreezing (fresh versus weathered snow surfaces). Anions also exhibit more variability than cations. Consequently, the parameter α is currently determined through calibration. Recently added capabilities to the standalone model include (1) the ability to add chemical inputs from rain-on-snow (ROS) events and (2) the effect of freezing or refreezing on chemical exchange between water phases, and (3) overwinter snow accumulation as opposed to only melt as in the original version of the model. The model has been successfully applied in the Arctic and Alpine regions of Canada and the USA (Costa et al., 2018, 2020). The model is available in public repositories (MATLAB version: <https://github.com/ue-hydro/PULSE>; C++ version: https://github.com/ue-hydro/PULSE_cpp).

2.2. Coupling PULSE to snowpack models

The PULSE model has been coupled to two snow-energy balance models, the double-snowpack layer Cold Regions Hydrological Model (CRHM, Pomeroy et al., 2022, 2007) and the multi-layer snowpack model (SNOWPACK, Lehning et al., 2002). The objective of having these two specific model coupling is to allow exploring the effect of considering a simpler 2-layer model versus a multilayer modelling approach resolving liquid water movement through layered snow using a van Genuchten formulation with retention curves tailored for snow. This approach also enables model intercomparison and helps identify key hydrological drivers and modelling needs required to improve the spatiotemporal predictability of seasonal snow chemistry. Other

snow-energy models should potentially be considered for integration with PULSE in the future (e.g., Leroux and Pomeroy, 2019). Fig. 2 shows how the coupling of PULSE was performed for both models, including the key model code files, the processes represented and the state-variables affected. In both cases, CRHM-PULSE and SNOWPACK-PULSE, the coupling is one-way, from the snow-energy balance models to PULSE, as ionic concentrations are not known to strongly affect snowpack energy and water-mass balances, as typically seen in other environments such as estuaries where the mixing of ocean and freshwater leads to density/gravity-driven flow. More details about the model couplings are provided in the following sections.

2.2.1. Coupling of PULSE to CRHM

CRHM is a modular physically based hydrological model that incorporates algorithms to model hydrological processes of considerable uncertainty for cold regions such as blowing snow, snow interception in forest canopies, sublimation, snowmelt, infiltration into frozen soils, hillslope water movement over permafrost, actual evaporation, and radiation exchange to complex surfaces (Pomeroy et al., 2007, 2022). It estimates the radiant energy terms and calculates blowing snow erosion and deposition from wind transport and sublimation using an implementation of the Prairie Blowing Snow Model (PBSM, Pomeroy and Li, 2000). Radiant transfer, stability corrected turbulent transfer, internal energy, ground heat flux, meltwater discharge and the solid and liquid mass balance of the snowpack are calculated using the Snobal snowpack module that is based on two layers, an upper exchange layer set to 10 cm and a deeper layer. The albedo module used the albedo decay routine of Verseghy (1991) that is deployed in several other models, including the Canadian Land Surface Scheme (CLASS) and others. The main output variables of CRHM used to drive the PULSE chemistry model are snow water equivalent (SWE), snow depth, and snowpack-surface snowmelt rates. The model has been successfully applied in many cold regions around the world, including Canada, China, Spain, Chile and Germany (Pomeroy et al., 2022).

The coupling of PULSE to CRHM is an external one and has been explained by Costa et al. (2018). In summary, PULSE takes modelled snowmelt data at the top of the snowpack from CRHM and then uses its own standalone implementation of the advection-diffusion equation for porous material to propagate the meltwater through the multilayer snowpack (Eq. (4)).

$$\frac{\partial(\theta_m c_m)}{\partial t} + \nabla \cdot (\theta_m \vec{v} c_m) = \nabla \cdot (\theta_m D \nabla c_m) + E \cdot \theta_{ss} \quad (4)$$

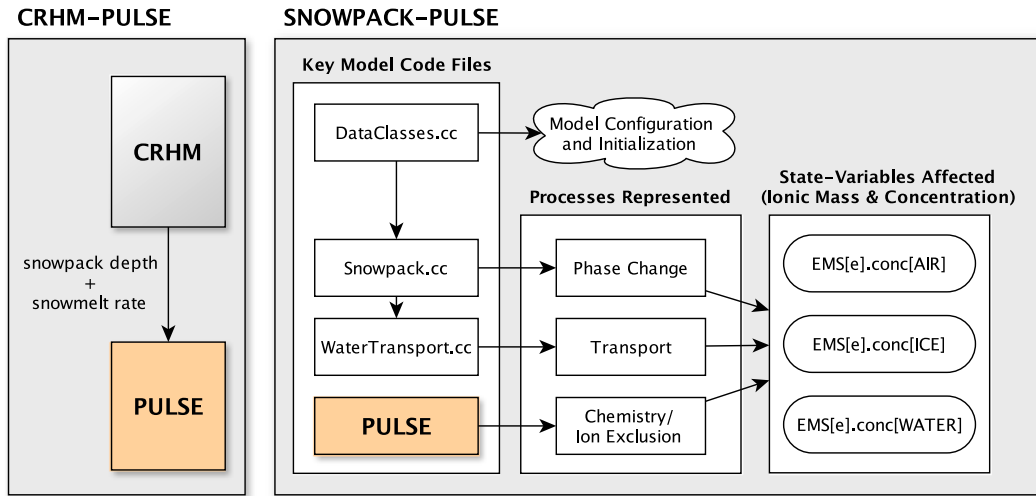


Fig. 2. Flowchart of the two model couplings. CRHM and PULSE were linked through external coupling so the models were run separately with the outputs of CRHM used as inputs for PULSE (left panel). This is the workflow originally designed for PULSE (Costa et al., 2018). SNOWPACK and PULSE were linked through internal coupling, so here the two models interacted throughout the simulation (right panel). The diagram identifies the key SNOWPACK model code files used for the coupling relating them to the respective processes and affected state-variables.

where $\nabla(\vec{v}c_m)$ describes advection, \vec{v} is the interstitial flow velocity (used as a proxy for the wetting front), D is the diffusion coefficient, $\nabla \cdot (D\nabla c_m)$ describes diffusion, and E represents the mass exchange between the percolating meltwater (liquid phase) and the snow grain surface as it melts (Eq. (3)). In the horizontal-averaged domain, the advection and diffusion terms can be written as

$$\nabla(\theta_m \vec{v}c_m) = \frac{\partial(\theta_m v c_m)}{\partial z} \quad (5)$$

$$\nabla \cdot (\theta_m D \nabla c_m) = \frac{\partial^2(\theta_m D c_m)}{\partial z^2} \quad (6)$$

The interstitial velocity is described as

$$v = q/\theta_m, \quad (7)$$

where q is the snowmelt rate. To calculate the dispersion coefficient (D), a simple approach often adopted in subsurface hydrology is used; dispersivity (d) is taken as a calibrated coefficient parameter to relate interstitial velocity (v) to D (Charbeneau et al., 1992),

$$D = d \cdot v \quad (8)$$

2.2.2. Coupling of PULSE to SNOWPACK

The use of the advection–diffusion in the CRHM-PULSE coupling version is a simplification which does not take into account internal snow processes, including refreezing of meltwater within the snowpack forming ice lenses, liquid water movement and capillary effects, which affect solute transport through the snowpack. Here, SNOWPACK was used to enable explicitly representing such processes, and coupled it to PULSE to investigate if such enhancements would translate into better snow chemistry predictions.

The snow cover model SNOWPACK (Lehning et al., 2002) was initially created to support avalanche warnings but has since expanded to other uses and applied in various cold regions, including Switzerland Schmucki et al. (2014), Canada and the Arctic (Ouellet et al., 2017), and Antarctica (Keenan et al., 2021). SNOWPACK simulates the layering and microstructure of snow by modelling energy and mass flow. It employs a Lagrangian finite element method to solve mass conservation equations for vapour and water phases, as well as temperature diffusion and momentum equations for the ice phase. The model considers the mechanical and physical properties of snow, such as thermal conductivity and viscosity, snow metamorphism, and

its interaction with the atmospheric boundary layer and penetrating shortwave radiation. The intricate texture of snow is characterized using four primary microstructure parameters: grain size, bond size, dendricity, and sphericity. The main variables of SNOWPACK used to drive the PULSE chemistry model (the models are internally coupled) are the spatiotemporal evolution of interstitial flow through snow and snow microstructure.

An important aspect of SNOWPACK that aims to enhance chemistry simulations with PULSE is its representation of liquid water movement through layered snowpacks, based on Darcy's law (Eq. (9)) and coupled with water retention curves tailored for snow using the van Genuchten formulation (Eq. (10)) (Hirashima et al., 2010). The unsaturated hydraulic conductivity is calculated according to Eq. (11). These water retention curves were derived from gravity drainage column experiments. The simulations aim to capture the capillary barrier that forms between layers of different grain sizes, such as the water-saturated layer at the interface between fine and very coarse snow.

$$q = K \left(\frac{dh}{dz} + 1 \right) \quad (9)$$

$$h = \frac{1}{\alpha} \left(\theta^{-1/m} - 1 \right)^{1/n}, \text{ where } m=1-1/n \text{ (} 0 < m < 1 \text{)} \quad (10)$$

$$K_r = \theta^{0.5} \left[1 - \left(1 - \theta^{1/m} \right)^m \right]^2 \quad (11)$$

where α and n are the parameters used to estimate the measured moisture characteristics curve. These parameters are calculated using Eqs. (12) and (13), which result in the behaviour shown in Fig. 3.

$$\alpha = 7.3 \times d + 1.9 \quad (12)$$

$$n = 15.68 \exp(-0.46d) + 1 \quad (13)$$

where d is the snow grain size computed dynamically by the model.

Since the movement of flow through the snowpack is explicitly simulated by SNOWPACK, PULSE does not use here the advection–diffusion equation to simulate the transport of dissolved substances. Instead, it used a simpler advection scheme deployed within the SNOWPACK-PULSE coupler (Eq. (14)).

$$\frac{\partial(\theta_m c_m)}{\partial t} + \nabla(\theta_m \vec{v}c_m) = E \cdot \theta_{ss} \quad (14)$$

The core conceptual model of PULSE (Fig. 1) and snow-core to snow-surface interactions remained as in the original model (Eqs. (1) and (2)).

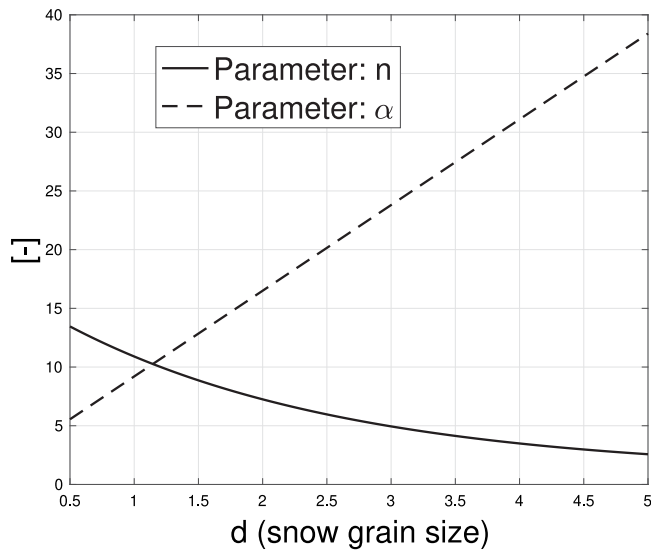


Fig. 3. Behaviour of the n and α parameters for the dynamic calculation of unsaturated hydraulic conductivity using Van Genuchten formulation.

2.3. Study site

The study region is located in the peninsula of Oscar II Land of the Spitsbergen island, Svalbard archipelago, Norway (Fig. 4). It is situated within the Bayelva river basin between Zeppelinfjellet and Scheteligfjellet, and north of Brøggerhalvøya, specifically 2 km southwest of the center of Ny-Ålesund and 1.21 km from the Hamnerabben Airport (Yuan et al., 2010; Boike et al., 2018). Ny-Ålesund comprises rich tundra vegetation and biodiversity. Vegetation covers 50 to 60% of the site, and the rest of the area is covered by stones and rock fields (Boike et al., 2018). Moraines, riverbed, tundra, and rock are important soil descriptors of the area (Kane and Yang, 2004). The geology is characterized by a pile of thrust sheets of Permo-Carboniferous siliciclastic (sandstones and conglomerates) to carbonate (limestones and dolostones) rock formations with alternating shale levels (Dagsson-Waldhauserova and Meinander, 2019).

The climate in Svalbard is characterized by rapid meteorological oscillations largely due to its geographical location and its exposure to the Gulf stream. Polar conditions (low temperature, dry air) are common throughout the year, particular during the winter, but can rapidly change (within a day) to maritime-type conditions with relatively higher temperature (sometimes reaching a few degrees above zero) and high relative humidity. These rapid oscillations can cause Rain-on-Snow (ROS) events that may produce ice layers and melt refrozen strata within the snowpack. These layers strongly affect the microstructure and permeability of the snowpack, promoting the development of preferential flow channels. The frequency of ROS events is expected to increase in the archipelago within the next decades due to warming conditions.

The specific location of the site used in this study (red empty square in Fig. 4) is in close proximity to the Bayelva Permafrost Station (BS) managed by the Alfred Wegener Institute (red circle labelled “BS” in Fig. 4). The average air temperature recorded in this station ranges between $-17\text{ }^{\circ}\text{C}$ and $-3.8\text{ }^{\circ}\text{C}$ in February and between $4.6\text{ }^{\circ}\text{C}$ and $6.9\text{ }^{\circ}\text{C}$ in June. The mean permafrost temperature recorded between 2009 and 2017 was $-2.3\text{ }^{\circ}\text{C}$, with a 5.5 m zero-amplitude depth (Boike et al., 2018). Although the region is characterized by stable stratification of air masses, low temperatures, and hence low water vapour content (Kühnel et al., 2011), which are unfavourable for the occurrence of precipitation, temperature gradients between a warmer sea and Ny-Ålesund contribute to substantial snowfall at the study site. It receives

an annual average precipitation of 400 mm as snow (Boike et al., 2018), but the annual precipitation can vary substantially, between 190 and 525 mm based on records from the 1960–1990 period, and the highest snowfall events often occur in early fall and cease in the winter when temperatures are lower.

2.4. Data description

Observations from two weather stations were combined to generate the meteorological dataset needed to drive the models, which included air temperature (T_{air}), relative humidity (RH), wind speed (WS), wind direction (WD), solar radiation (RAD), and precipitation (PREC in mm). The stations are the Bayelva Permafrost Station (BS) and the Ny-Ålesund station. The locations are depicted in Fig. 4. The Bayelva station is located at the high Arctic permafrost research site in Spitsbergen, which is 26 m above sea level at the top of the Leirhaugen hill. Data from this station was obtained from Boike et al. (2018) and is available at <https://zenodo.org/record/1139714> The Ny-Ålesund station (SN9910) is located north-western of Spitsbergen and is managed by the Norwegian Meteorological Institute. Data for this station was obtained via the official data repository named “KLIMA” (eklima.met.no).

Since this research expands from previous inter-annual snowpack modelling work using CRHM that used hourly data from the Bayelva station for the 1992–2013 period (López-Moreno et al., 2016), the same dataset used and extended through 2017 using data from the same station obtained from Boike et al. (2018). Data from the Ny-Ålesund station was used to complete the meteorological timeseries. The respective sources used for each meteorological variable are shown in Fig. 5.

Previous work has highlighted that the case study is located in an area subject to high wind-induced precipitation undercatch (Pollock et al., 2018; López-Moreno et al., 2016). Errors associated with different snow gauges have been identified as both instrumental and environmental (Pollock et al., 2018). Snowfall undercatch due to wind or Alter shielded precipitation gauges was estimated by Smith et al. (2020) to correct the measurement. The reader is referred to López-Moreno et al. (2016) for more information about this correction. Snowpack depths between 1997 and 2010 were obtained from the Bayelva station and used to validate the snow accumulation, redistribution and ablation models. Detailed vertical profiles of snowpack chemistry were collected by the National Research Council of Italy (CRN) throughout the snow accumulation and ablation periods of 2015. The in-snow measurements included temperature, as well as major anions and cations, including nitrate (NO_3^-), sulfate (SO_4^{2-}), potassium (K^+), magnesium (Mg^{2+}), chlorine (Cl^-), calcium (Ca^{2+}), and bromine (Br^-). The chemistry data was used to verify the model performance.

Snow sampling and chemical analysis

Detailed snowpack chemical vertical profiles were obtained between the 27th of March to the 30th of May 2015 (Spolaor et al., 2021). Daily 1-m deep snow pits were dug perpendicular to the glacier ice flow and main wind direction pattern. The exposed snow walls were sampled using polyethylene pre-cleaned tubes with a depth resolution of 10 cm. After each daily sampling, the snow pit was carefully filled in, and an adjacent snow pit was dug approximately 30 cm away in the upwind direction on the following day. All snow-pits were collected inside an area of $10 \times 10\text{ m}$, and the samples were kept frozen until chemical analysis. The dataset has been previously used to investigate snowpack dynamics during rain and melting events (Spolaor et al., 2021). A full description of the annual snowpack evolution can be found in Spolaor et al. (2021, 2016).

The concentrations of sulfate (SO_4^{2-}), sodium (Na^+), and calcium (Ca^{2+}) were used to validate the model. They were determined using an ion chromatograph (Thermo Scientific™ Dionex™ ICS-5000, Waltham, US) coupled with a single quadrupole mass spectrometer (MSQ Plus™,

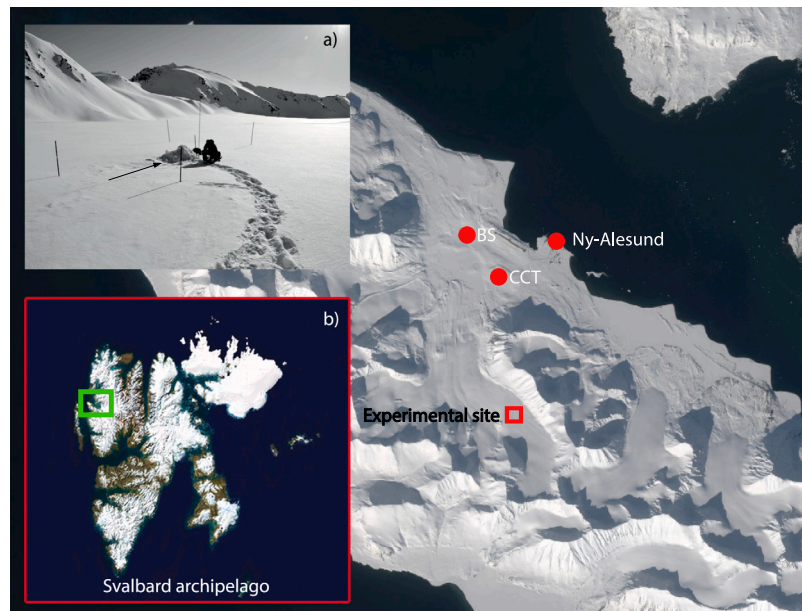


Fig. 4. Experimental study site (red empty square) located near the Bayelva Permafrost Station (red circle labelled “BS” ; 78.92094 N, 11.83334 E), the Ny-Ålesund station (red circle labelled with the station name), and the Amundsen Nobile Climate Change Tower (red circle labelled “CTT” ; 78.92141 N, 11.86630 E). The latter has not been used in this study. (For interpretation of the references to colour in this figure legend, the reader is referred to the web version of this article.)

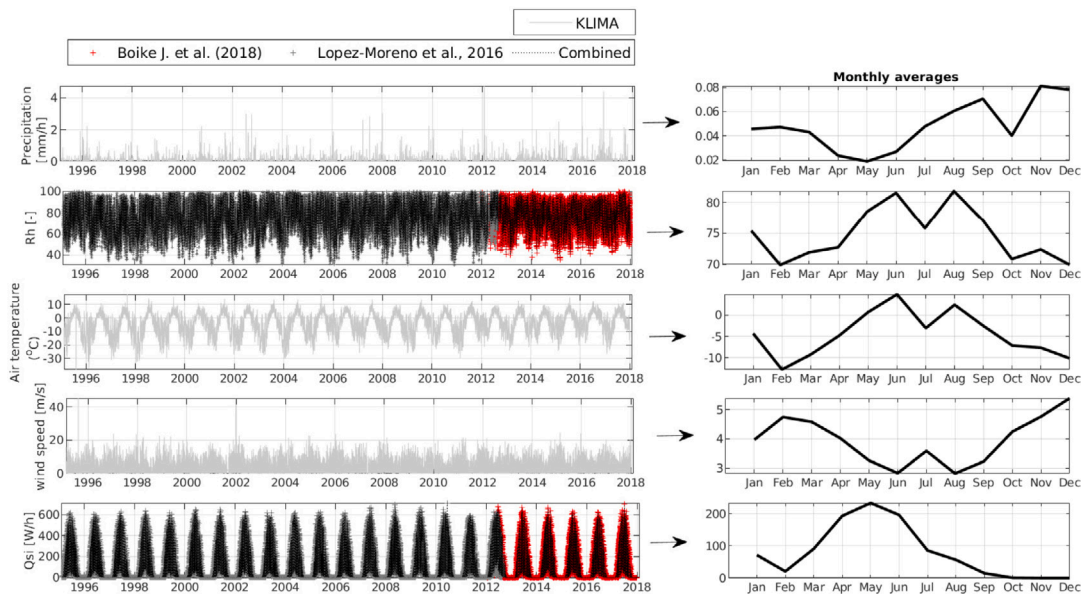


Fig. 5. Meteorological data combined from different sources and used to drive the models. Data from Boike et al. (2018) and López-Moreno et al. (2016) are from the Bayelva station. The “KLIMA” dataset corresponds to data from the Ny-Ålesund station.

Thermo Scientific™, Bremen, Germany). The analysis of SO_4^{2-} was performed using an anion exchange column and a guard column (Dionex Ion Pac AS11 2×250 mm and AG11 2×50 mm) through a gradient elution with sodium hydroxide as the mobile phase. The separation of cations was carried out using a capillary cation exchange column with a guard column (Ion Pac CS19-4 μm 0.4×250 mm and CG19-4 μm 0.4×50 mm) through a gradient elution with methanesulfonic acid as the mobile phase and a conductivity detector. A detailed description of the analytical measurements is provided in Barbaro et al. (2017).

The rain-on-snow event (ROS) - April 16th 2015

The period of the experiment was characterized by changing meteorological conditions that affected the seasonal snowpack microstructure. The initial period between the 27th of March and the 15th of

April experienced cold and stable air temperatures with no snowmelt. A ROS event occurred on April 16th. The following period between the 17th of April and the 15th of May was affected by this ROS event that produced a negative thermal gradient in the snowpack. A decrease in air temperature eventually restored the positive thermal snow gradient with “the cold” propagating into the deeper snow layers. The remaining period of the experiment was characterized by an initial warming until the snow temperature profile became quasi-isothermal and surficial snowmelt was initiated. The event is highlighted in Fig. 6 of Section 2.5.

2.5. Model application and validation

The two components of the coupled models, i.e., hydrology and chemistry, were both validated against observation data. First, the

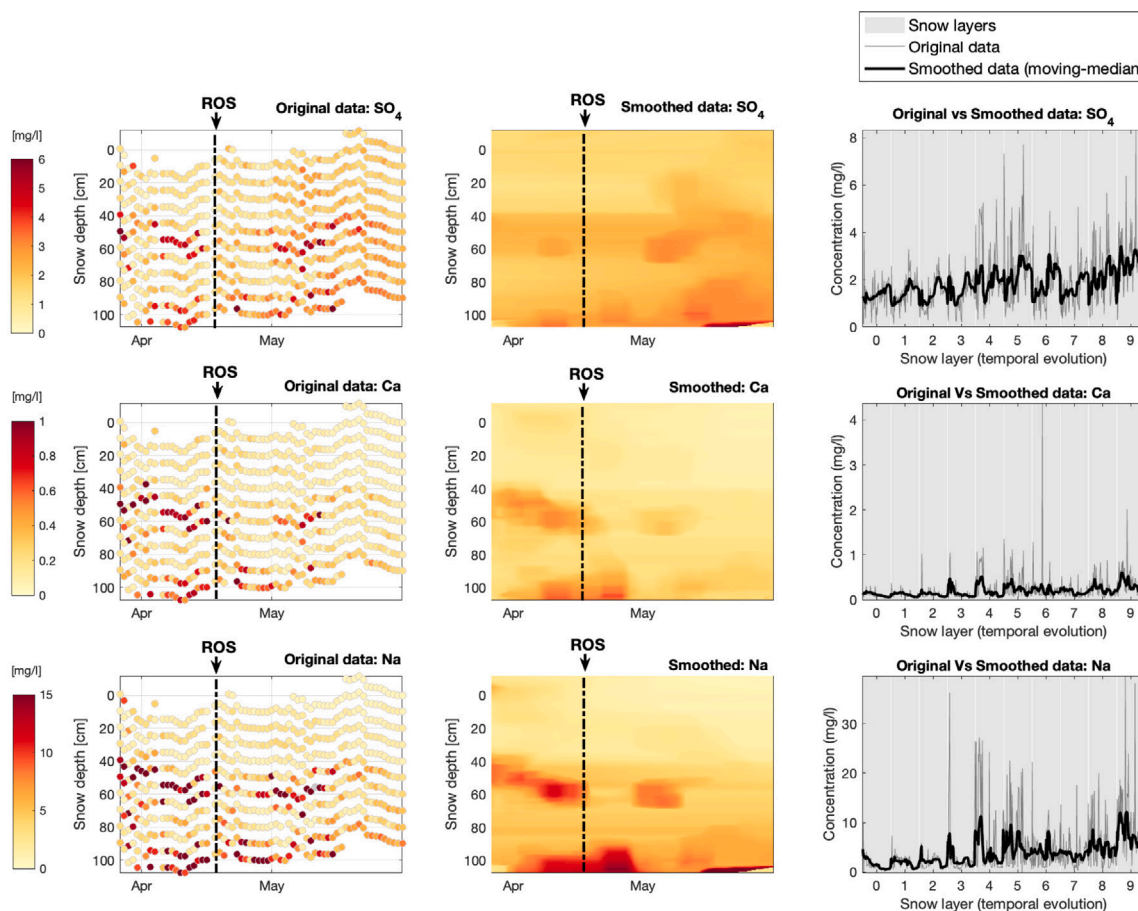


Fig. 6. Measured/original concentration distribution (left-column panels) and smoothed concentration distribution via moving-median (middle-column panels) measured in 2015. The right-column panels compare “original” (left-column panel) and “smoothed” (middle-column panel). The data in the right-column panels display the same information of the corresponding right- and middle-column panels but in a stacked format. In other words, the 2D time-space matrix was linearized by stacking the vertical concentration profiles across all time steps. This linearization was done to more clearly highlight the differences between the original and smoothed data.

hydrological component (i.e., CRHM and SNOWPACK) of each coupled model (CRHM–PULSE and SNOWPACK–PULSE) was validated using snow depth measurements collected between 1997 and 2010 (see details in Section 2.4). This was performed for the two hydrological models prior to initiating the chemistry simulations. Second, the chemistry component (i.e., PULSE) was verified for one year using detailed Na^+ , Ca^{2+} , and SO_4^{2-} vertical snowpack concentration profiles measured during the accumulation and ablation periods.

Meteorological data (see Section 2.4) was used to drive the hydrological component of the coupled models. These hydrological models were set up and parameterized using similar considerations, except for the number of snow layers, which was a key aspect of the investigation in this study and conjectured to impact the quality of the subsequent chemistry simulations. CRHM is a two-layer model, while SNOWPACK, a multi-layer snow model, was set up with 100 layers. The high snowpack vertical resolution in SNOWPACK was chosen to maximize the capturing of liquid water movement through the layered snow and its impact on chemistry. For the chemistry simulations with PULSE, a 100-layer discretization was adopted for both model couplings, which in the case of SNOWPACK directly linked to the layer-specific calculations, but in the case of CRHM, the layer-specific snow properties were estimated using PULSE’s original approach that is described in Section 2.1.

The parameterization of CRHM was taken from previous work developed for Svalbard by López-Moreno et al. (2016), where albedo of fresh snow was defined as 0.9, and that of aged snow was limited to 0.3. Blowing snow was activated in both models, although they use different approaches. The reader is referred to López-Moreno et al.

(2016) for more information about the uncalibrated CRHM model setup. CRHM’s approach for computing snow wind erosion is based on PBSM, which is briefly described in Section 2.2.1, while that used in SNOWPACK involves the calculation of suspended and saltation mass fluxes following Pomeroy and Gray (1990).

Due to limited data on wet and dry deposition rates of Na^+ , Ca^{2+} , and SO_4^{2-} in the case study area during the period of the chemistry simulation (2015), the ionic concentrations measured at the snowpack surface were used as a proxy for the concentrations of the input precipitation used to drive the chemistry model (PULSE). The high-resolution, daily snow chemistry profile data obtained from snowpits (see Section 2.4) was used to force (only the initial snow concentrations) and verify (remaining snow chemistry data) the performance of the coupled models. Previous research interpreting this chemistry profile data revealed challenges, which were attributed to the high layer variability and local effects caused by snowpit migration during sampling (Spolaor et al., 2016). The authors proposed smoothing the data to help reveal the key spatiotemporal patterns. This was carried out here using a space–time moving median, as shown in Fig. 6, particularly in the three panels of column three.

The selection of Na^+ , Ca^{2+} , and SO_4^{2-} for simulations was deliberate. Na^+ is the main component of the sea spray source in the atmosphere, and it is one of the most abundant ions in the Svalbard snowpack (29%–36% of the total loading) (Barbaro et al., 2021). Ca^{2+} is taken as an indicator of input of terrestrial dust, although it can have a minor contribution from sea salt. In Svalbard, the most likely non-sea-salt source is terrestrial dust derived from local rocks, which are free of snow during the warmest months. Dust is not evenly mixed

Table 1
Model configurations and relevant parameters (CRHM, SNOWPACK and PULSE)

Parameter	Value	Admissible range	Units	Description
CRHM (1999–2012): Hydrology and Snowpack dynamics				
<i>Albedo_Bare</i>	0.17	0 to 1	–	Albedo for bare soil (<i>albedo_Richard</i> module)
<i>Albedo_Snow</i>	0.85	0 to 1	–	Albedo for snowpack (<i>albedo_Richard</i> module)
<i>amax</i>	0.84	0 to 1	–	Maximum albedo for fresh snow (<i>albedo_Richard</i> module)
<i>amin</i>	0.5	0 to 1	–	Minimum albedo for aged snow (<i>albedo_Richard</i> module)
<i>smin</i>	1	0 to 20	mm/int	Minimum snowfall to refresh snow albedo (<i>albedo_Richard</i> module)
<i>a1</i>	1.08E+07	0 to 1E8	–	Albedo decay time constant for dry cold snow (<i>albedo_Richard</i> module)
<i>a2</i>	7.20E+05	0 to 1E8	–	Albedo decay time constant for melting snow (<i>albedo_Richard</i> module)
<i>hru_F_g</i>	0	–50 to 50	W/m ²	Depth of soil temperature measurement (<i>SnobalCRHM</i> module)
<i>hru_rho_snow</i>	100	50 to 1000	kg/m ³	Density of snowfall (<i>SnobalCRHM</i> module)
<i>max_h2o_vol</i>	0.01	0.0001 to 0.2	–	Max liquid h2o content as volume ratio: $V_{water}/(V_{snow} - V_{ice})$ (<i>SnobalCRHM</i> module)
<i>max_z_s_0</i>	0.1	0 to 0.35	m	Maximum active layer thickness (<i>SnobalCRHM</i> module)
SNOWPACK (1999–2012): Hydrology and Snowpack dynamics				
<i>α</i>	Eq. 14 and Fig. 3	–	–	Parameter for the dynamic calculation of unsaturated hydraulic conductivity using Van Genuchten formulation
<i>n</i>	Eq. 13 and Fig. 3	–	–	Parameter for the dynamic calculation of unsaturated hydraulic conductivity using Van Genuchten formulation
<i>ROUGHNESS_LENGTH</i>	0.002	–	m	Initial estimate of the roughness length for the site, but it is adjusted throughout the simulation
<i>GEO_HEAT</i>	0.06	–	W m ⁻²	Fixed geothermal heat flux (Van Neumann boundary condition)
<i>THRESH_RAIN</i>	1.2	–	°C	Temperature threshold for setting precipitation falling as rain
<i>HOAR_THRESH_TA</i>	1.2	–	°C	Temperature threshold for surface hoar destruction or formation
<i>HOAR_THRESH_RH</i>	0.97	–	°C	Relative humidity threshold for surface hoar destruction or formation
<i>HOAR_THRESH_YW</i>	3.5	–	°C	Wind speed threshold for surface hoar destruction or formation
<i>HOAR_DENSITY_BURIED</i>	125	–	kg/m ³	Density of BURIED surface hoar
<i>HOAR_MIN_SIZE_BURIED</i>	2	–	mm	Minimum surface hoar size to be buried
<i>HOAR_DENSITY_SURF</i>	100	–	kg/m ³	Density of surface hoar
<i>MIN_DEPTH_SUBSURF</i>	0.07	–	kg/m ³	Density of sub-surface hoar
<i>NEW_SNOW_GRAIN_SIZE</i>	0.3	–	m	Size of new snow rains
<i>METAMORPHISM_MODEL</i>	DEFAULT	–	–	Metamorphism model used
<i>VISCOSITY_MODEL</i>	DEFAULT	–	–	Viscosity module used
<i>SALTATION_MODEL</i>	SORENSEN	–	–	Saltation module used
<i>ALBEDO_AGING</i>	TRUE	–	–	Albedo aging considered
<i>SW_ABSORPTION_SCHEME</i>	MULTI_BAND	–	–	Computation of absorbed radiation
<i>HARDNESS_PARAMETERIZATION</i>	MONTI	–	–	Computation of hardness model
PULSE (2015): Chemistry dynamics				
<i>conc_0</i>	ISMVP ^a	–	mg/l	Initial snowpack concentrations
<i>conc_precip</i>	SMSS ^b	–	mg/l	Ionic concentration of precipitation (rain or snow)
<i>α</i>	2.00E–03	–	–	Snow ion exclusion coefficient
<i>d</i>	3.45E–07	–	–	Dispersivity (only applicable to CRHM-PULSE)

^a ISMVP: Initial snowpit measurements (vertical profile).

^b SMSS: Snowpit measurements at the snowpack surface.

in the air because the particle size is large, and transportation paths from the sources are relatively short (Virkkunen et al., 2007). SO₄²⁻ can come from primary and secondary sources. A minor contribution to the sulphate budget comes from sea salt (Spolaor et al., 2021), while the dominant fraction can have anthropogenic or biogenic sources. Biogenic sulphate, typically predominant from April onward (Ardyna et al., 2013; Spolaor et al., 2021), can occur in the snow as an oxidized by-product of dimethyl sulphide (DMS) emitted by marine algal blooms (Gondwe et al., 2003). Another plausible source in Svalbard is the long-range atmospheric transport of secondary aerosols containing ammonium sulphate. This can be formed by SO_x emitted from coal combustion throughout the winter and biomass burning in the spring (Nawrot et al., 2016).

The chemistry component of the model was manually set up for each of the ions simulated since ion exclusion rates vary between ions as described in Costa et al. (2018, 2020). This calibration involved defining two parameters, (1) a chemical dispersion coefficient (D, m/s), an ion exclusion coefficient (α). The reader is referred to Section 2.1 and Costa et al. (2018) for more details about the PULSE model. Simulations were performed at hourly time steps in both coupled models (CRHM–PULSE and SNOWPACK–PULSE). The model performances were evaluated using the Root-Mean-Square Error (RMSE, Eq. (15)) and Model Bias (MB, Eq. (16)). Table 1 summarizes some of the model parameters and configurations used. Additional information can be found in Table 1

and the model public repositories.

$$RMSE = \sqrt{\frac{\sum_{i=1}^N (X_i^{obs} - X_i^{mod})^2}{N}} \quad (15)$$

$$MB = \frac{\sum_{i=1}^N X_i^{obs}}{\sum_{i=1}^N X_i^{mod}} - 1 \quad (16)$$

where N is the number of observations available for model validation and X_i^{obs} and X_i^{mod} are the observed and simulated variable values.

3. Results

3.1. Snow hydrology: 1999–2012

Observed and simulated snowpack depths obtained with the hydrological components of both coupled models (CRHM and SNOWPACK) are compared in Fig. 7 for a 13-year period (1999–2012). The simulation results generally agree well with the observations for both models on either the calibration (only applicable to SNOWPACK) or validation periods. CRHM was not calibrated as described in López-Moreno et al. (2016), but parameters were set from scientific knowledge. The first year (1998) was used for simulation warm-up and the subsequent three years (1999–2001, 3 years) were used to guide the parameterization of

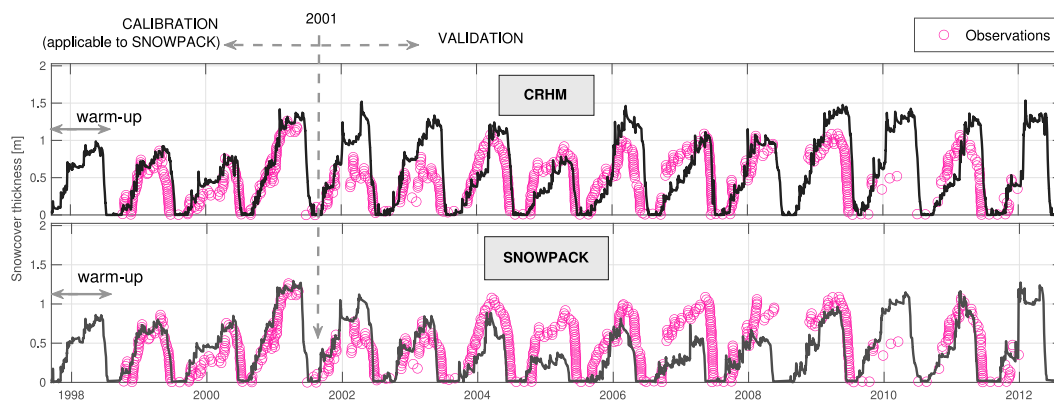
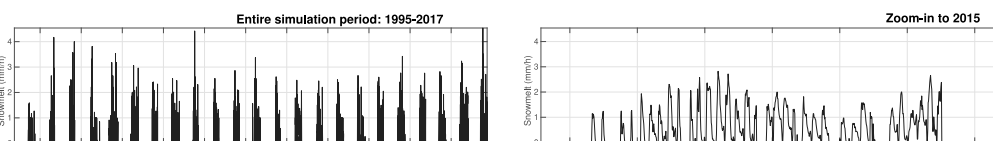
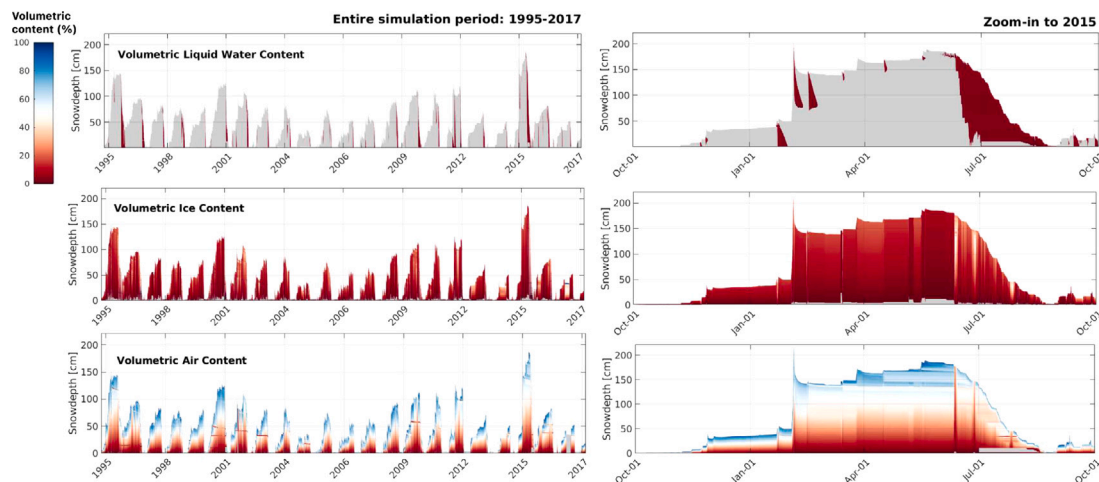


Fig. 7. Observed and simulated snowdepth using the CRHM (upper panel) and SNOWPACK (lower panel) models.



(a) CRHM: snowmelt rates (1995-2017)



(b) SNOWPACK: Volumetric content for liquid water, ice, and air

Fig. 8. Hydrological results calculated by CRHM (panel a) and SNOWPACK (panel b) used to drive PULSE.

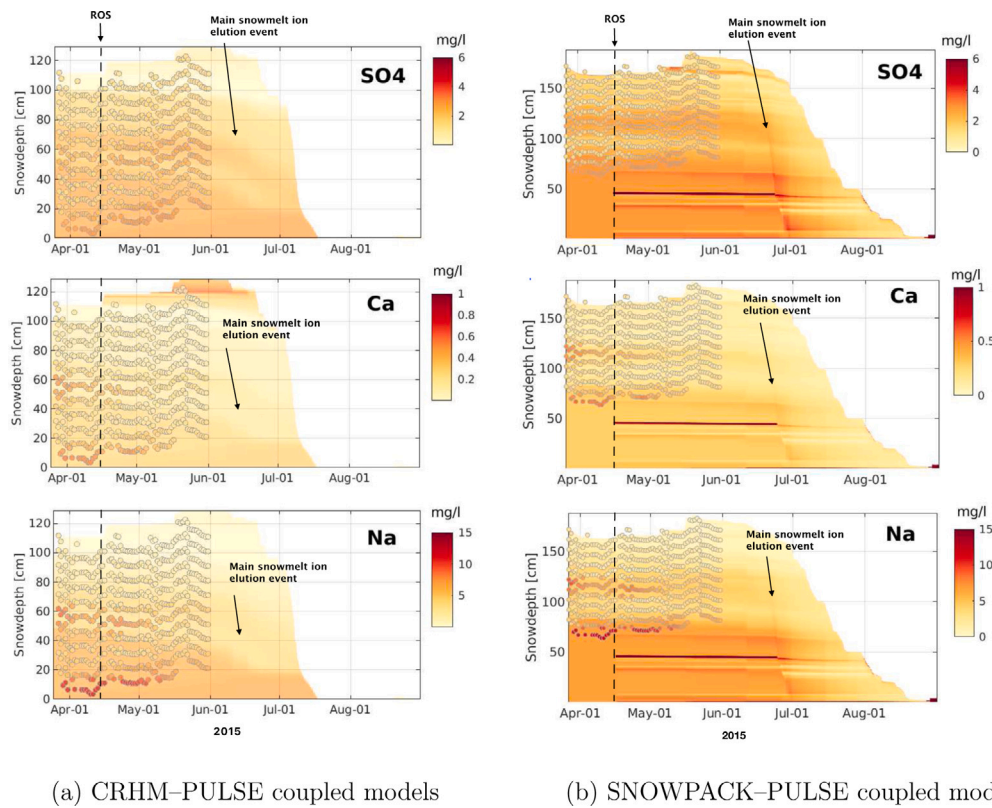
SNOWPACK. The validation period (2002–2012, 10 years) is substantially larger than the calibration one to ensure the model performance assessment captures a wide variety of meteorological conditions. Section 3.3 provides more details about the performance of the coupled models, but a few particular years where models performed worse are worth noting here. In the case of SNOWPACK, snowpack depth was underestimated by about 50% in 2005 and 35%–40% in 2007. In the case of CRHM, the peak snowpack depth was overestimated by about 50% in 2002 and 30% by 2003.

Although identifying the exact causes for the mismatch in these specific years is difficult, possible causes may include issues with the meteorological input data, such as (1) precipitation undercatch, (2) inconsistencies between the data combined from the three weather stations used, (3) the distance of the experimental site to the weather stations, and (4) differences in the precipitation phase and blowing snow schemes, modelling assumptions and model setup. It should be noted that previous research has highlighted challenges in examining and simulating snowpack evolution in the Arctic due to its uneven wind spatial redistribution, particularly in open tundra (López-Moreno

et al., 2016; Pomeroy and Li, 2000). It should be noted that although similar parameter considerations were used to set up both models, these models are intrinsically and structurally different in many ways. For example, CRHM uses a two-layer snowpack model while SNOWPACK is a multi-layer snowpack model. Also, CRHM simulates the entire hydrological cycle while SNOWPACK focuses on the snowpack.

3.2. Snow hydrochemistry: 2015

Fig. 8 shows the hydrological and thermodynamic conditions obtained with CRHM (panel a-right) and SNOWPACK (panel b-right) for 2015, which were used to drive the snowpack chemical response with PULSE (the chemical model component). Because CRHM uses a two-layer snowpack module, while SNOWPACK is a multi-layer snowpack model, the type of hydrological model outputs used to initiate and force PULSE were different. In the case of CRHM–PULSE, only surface snowpack snowmelt rates (panel b-right) were available to drive the chemistry simulations. Here the original, simple approach deployed in PULSE to dynamically estimate interstitial flow velocities



(a) CRHM–PULSE coupled models

(b) SNOWPACK–PULSE coupled models

Fig. 9. Observed (coloured circles) and simulated (background coloured surface) snowpack concentrations using the CRHM–PULSE and SNOWPACK–PULSE coupled models for SO_4^{2-} , Ca^{2+} and Na^+ . The snowdepths are different (left and right panels) because CRHM and SNOWPACK produced different snowpack depths in 2015 (max predicted depth was ~ 125 cm with CRHM and 155 cm with SNOWPACK). Since the snowpit chemistry observations were taken using the snowpack top surface as the reference for the measurement locations, they are displayed here using a similar approach using the simulated snowpack surface as the reference, which is different for each of the models. (For interpretation of the references to colour in this figure legend, the reader is referred to the web version of this article.)

was used (see Section 2.1 and Costa et al. (2018)). In the case of SNOWPACK–PULSE, the internal microstructures across the snowpack profile are simulated, including the volumetric ice, water and air content, and liquid water fluxes (panel b-left). Therefore, PULSE was internally coupled to SNOWPACK to benefit from additional detail on micro-flow spatiotemporal patterns, which allowed refining in-snow hydro-chemical transport calculations and the impact of phase changes and snow layering.

Fig. 9 compares observed and simulated snow chemistry for SO_4^{2-} , Ca^{2+} and Na^+ . CRHM and SNOWPACK produced different snowpack depths in 2015 (max predicted depth was ~ 125 cm with CRHM and 155 cm with SNOWPACK), and the snowpit chemistry data was measured extending 1 m from the snowpack surface (see Fig. 9). Both model and observations show the development of snowpack layers with different concentrations as a result of (1) seasonal changes in chemical wet and dry deposition and (2) snow layering where phase and snow density changes affect chemical concentrations. Results show that ROS events and snowmelt strongly affect the vertical distribution of chemicals and are responsible for the migration of chemicals deeper into the snowpack, where refreezing may occur. These layers are more pronounced in the SNOWPACK–PULSE simulations because the snowpack microstructure is explicitly resolved.

3.3. Performance of coupled models: hydrology and chemistry

Observed and simulated SO_4^{2-} , Ca^{2+} , and Na^+ concentrations obtained with CRHM–PULSE and SNOWPACK–PULSE are compared in Fig. 10. Table 2 shows the performance of the coupled models for both hydrological and chemical variables. For PULSE, results obtained when disabling PULSE’s snow ion exclusion (SIE) module are also included. The uncalibrated CRHM performed slightly better with a lower RMSE

Table 2

Model performance for snowdepth and SO_4^{2-} , Ca^{2+} and Na^+ concentrations based on RMSE and mean bias. SIE refers to snow ion exclusion.

State-variable (hydrology)	Model	RMSE [m]	Bias [-]
Snowdepth	CRHM	0.30	-0.18
	SNOWPACK	0.28	0.11
State-variable (chemistry)	Model	RMSE [mg/l]	Bias [-]
SO_4^{2-}	CRHM (with SIE)	0.72	0.04
	CRHM (without SIE)	0.72	0.04
	SNOWPACK (with SIE)	0.64	-0.11
	SNOWPACK (without SIE)	0.64	-0.12
Ca^{2+}	CRHM (with SIE)	0.11	0.29
	CRHM (without SIE)	0.11	0.29
	SNOWPACK (with SIE)	0.09	0.28
	SNOWPACK (without SIE)	0.09	0.26
Na^+	CRHM (with SIE)	2.01	0.15
	CRHM (without SIE)	2.01	0.15
	SNOWPACK (with SIE)	1.50	0.07
	SNOWPACK (without SIE)	1.50	0.07

for the predicted snowdepth than the calibrated SNOWPACK, a difference that is visually noticeable in Fig. 7. Both Fig. 10 and Table 2 show that both coupled models are able to reproduce the general patterns of the temporal vertical evolution of concentrations of the simulated ions in the snowpack.

SNOWPACK–PULSE shows better performances, likely due to SNOWPACK providing a multi-layered representation of the evolution of vertical density changes and interstitial flow velocities that strongly affect solute transport, unlike CRHM that is a hydrological model that deploys a simpler two-layer snowpack representation. Recall that in CRHM–PULSE (externally coupled), the original PULSE approach

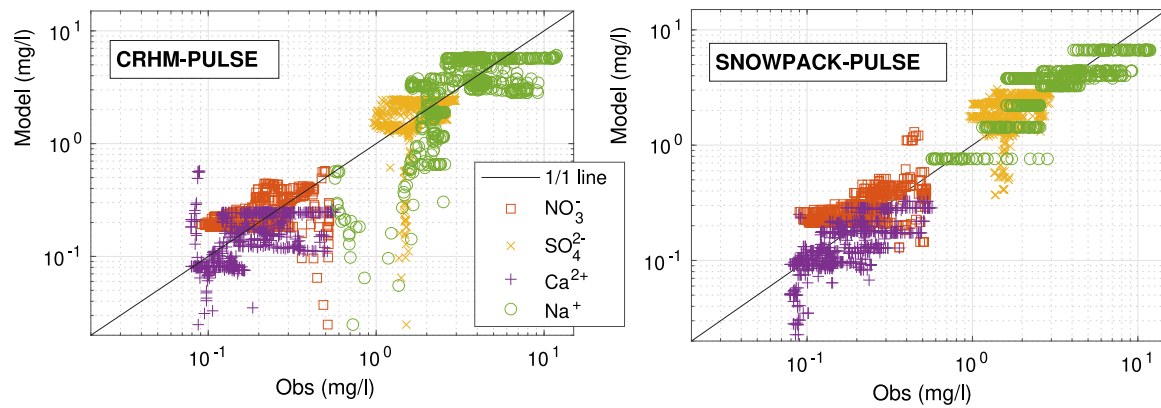


Fig. 10. CRHM-PULSE and SNOWPACK-PULSE model performance for hydrology and chemistry.

for estimating interstitial flow velocities is dynamic but indirectly estimated through a simplified method based on melt rate and depth-integrated snowpack porosity (see Costa et al., 2018). Despite some uncertainty in the predictions, results show that the models are able to generally predict concentrations across different orders of magnitude (10^{-2} to 10 mg/l). A major challenge with coupled hydrological-chemical simulations is the propagation of uncertainty and errors between models (from hydrology to chemistry). In the particular case of snowpack simulations, the simulated evolution of interstitial flow pathways, timing, and intensity significantly impact the prediction of spatiotemporal chemical distributions. Also, although the chemical constituents simulated (biologically emitted (SO_4^{2-}), dust particles (Ca^{2+}), and sea salt (Na^+)) are considered stable in cold snowpacks (i.e., subject to limited biogeochemical cycling), temporary changes in air temperature may also lead to a slight increase in bio-mediated processes.

4. Discussion

4.1. Snow chemistry sampling: lessons from modelling for capturing key spatiotemporal patterns and drivers

The seasonal snow cover can strongly affect streamflow and water quality, soil temperature and permafrost, and glacier mass balance, which may have an impact on the hydrological cycle and carbon exchange dynamics in cold regions (Larose et al., 2013b). The predicted warming of air temperatures at lower latitudes has effects on contaminants through increased volatility and altered partitioning between phases, whereas increased precipitation could lead to more mixing and removing of contaminants by rain and snow (Larose et al., 2013a; Costa and Pomeroy, 2019; Costa et al., 2019).

The high-resolution snowpack chemical profiles used in our study were obtained via an experiment performed in the spring period of 2015 by Spolaor et al. (2016, 2021). The archipelago of Svalbard is characterized by a maritime climate with large, rapid temperature variations during winter (Hansen et al., 2014). This experiment demonstrated that such changing meteorological conditions strongly affect seasonal snowpack microstructure, layering and redistribution of solutes (see Fig. 6). The meteorological conditions recorded during the experiment included a ROS event that produced a negative thermal gradient, which was reversed following a decrease in air temperature. Later, warming led to quasi-isothermal conditions and the initiation of melt.

Spolaor et al. (2016) highlighted challenges in interpreting the evolution of the vertical chemistry profile data collected. High spatial variability and local effects were attributed as key causes for some unexpected rapid changes in concentrations - see left and right panels of Fig. 6. However, smoothing of the data proved to be a useful approach

to reveal the key spatiotemporal patterns in the past (Spolaor et al., 2016) and in the herein study as well (left and middle panels of Fig. 6). The initial application of the two coupled hydrology-chemistry models (CRHM-PULSE and SNOWPACK-PULSE) experienced difficulties in explaining the chemical evolution of the snowpack without the smoothing of the observation results (see Fig. 9). This highlights the high heterogeneity and complexity of snowpack chemistry, which calls more research in this area and continuous high-resolution, high-frequency monitoring programs. Such data will be critical to advance further process understanding, model predictions, and the anticipation of climate change impacts.

4.2. Key moments in winter snowpack chemistry

Seasonal snow cover is expected to become more unstable in the future. Continuous air temperature increase is predicted to produce shorter snow seasons and increase the frequency of ROS events (Beniston and Stoffel, 2016; Morán-Tejeda et al., 2016). However, recent studies have highlighted the critical need to reduce uncertainty in capturing changes in precipitation to enable more reliable predictions of the impacts on snowpacks (e.g., López-Moreno et al., 2009). Past studies on preferential ionic elution in melting snowpacks have shown that 50%–80% of the total snow ion mass can be transported during the initial 1/3 of meltwater (Brimblecombe et al., 1986; Marsh and Pomeroy, 1999; Costa and Pomeroy, 2019). ROS events are known to promote the formation of preferential flowpaths (PFP) in snowpacks, affecting snowpack discharge. Preferential flow leads to accelerated percolation and solvent concentration in meltwater (Larose et al., 2013a). In a lab experiment using high-frequency flow and chemistry measurements, Costa and Pomeroy (2019) found that snowpack flow fingering (i.e., preferential flowpaths), which naturally develops in melting snowpacks, released more than 20% of the total NO_3^- and PO_4^{3-} snowpack load during the first 1.5% of snowmelt. However, ROS reduced the magnitude of this early load to 5% and 12% of the total NO_3^- and PO_4^{3-} snow load. It was hypothesized that ROS forced rapid flow through specific preferential flowpaths providing less opportunity for the wash-up of chemicals from the entire snowpack.

The observations (Fig. 6) and model results (Fig. 9) presented in this study showed that ROS and snowmelt had a disproportionate effect on the vertical redistribution of snow ions, characterized mainly by downward transport, melting and refreezing, dilution, and dispersion. Both coupled models were able to generally capture these key moments. However, SNOWPACK-PULSE showed a better performance likely due to SNOWPACK providing a more detailed and dynamic representation of vertical interstitial flow affecting chemical transport. Concentration changes observed in the measurements during cold periods could not be entirely explained by the mass-balance approaches provided by CRHM-PULSE and SNOWPACK-PULSE. These changes are likely to be

caused by snow redistribution by wind and associated snow chemistry changes (Pomeroy et al., 1991), as well as local effects and spatial heterogeneity during sampling. Recall that after each daily sampling, the snow pit was carefully filled in, and an adjacent snow pit had to be dug on the following day approximately 30 cm away in the upwind direction (see). Future research should continue to shed light on these heterogeneous contaminant accumulation and release processes, identifying the critical additional biogeochemical and biological process model representation needs to improve simulation predictions.

4.3. Science-modelling gaps and future research

The increase in ROS events has consequences for the chemical composition of the snow, including contaminants that are trapped/deposited in the snowpack during the winter. ROS events can cause the early release of pollutants from the snowpack into both the ground and seawater/fjord, especially if the event is intense enough to start the hydrological system of the area surrounding Ny-Ålesund (Salzano et al., 2023). Continuing to further improve our understanding of snow chemistry and elution of pollutants during such ROS requires continuing progress in both terms of data collection and prediction capacity.

Also, non-biological overwinter chemical changes in cold Arctic snowpacks have been observed before and were associated with temperature gradient metamorphism, which sublimates the original crystals and reforms them as depth hoar (Pomeroy et al., 1993). This reduces the snowpack density and promotes vapour transport, and associated solute movement, from the snowpack. Although a slow process, this transport mechanism is persistent throughout the winter and excludes Ca^{2+} , Cl^- , and SO_4^{2-} , which accumulate in the snowpack leading to an increase in concentrations. Although such processes are accounted for in CRHM and SNOWPACK, thus affecting chemistry simulations with PULSE, it remains a challenging process to simulate. Additional processes that require further research and model advances include (1) the effect of blowing snow and sublimation on snow erosion and deposition, and associated solute balance (Pomeroy et al., 1991), (2) potential photochemical reactions which would be prevalent in spring before melt (Jones et al., 1993), and (3) preferential flow path formation (Leroux and Pomeroy, 2017) and impacts on solute transport (Costa and Pomeroy, 2019).

5. Conclusions

The PULSE snow model has been coupled to two energy-balance snowpack models, the Cold Regions Hydrological Model (CRHM) and the SNOWPACK model, to simulate the spatiotemporal evolution of snowpack chemistry in Svalbard, Norway. The study aimed to help advance the current prediction capacity for snowpack chemistry to help anticipate the effect of rapid winter air temperature oscillations and frequency of ROS events on snowpack microstructure, hydrology and chemistry.

Both CHRM-PULSE and SNOWPACK-PULSE could capture snow depths accurately in the study site between 1999 and 2012. High-resolution snowpack chemistry profile data previously collected at the site was used to validate the coupled models for Na^+ , Ca^{2+} and SO_4^{2-} . Both coupled models were able to generally capture the main patterns and evolution of winter snowpack chemistry profiles, including the effects of rain-on-snow and snowmelt. However, SNOWPACK-PULSE that provides a multi-layered representation of vertical phase changes and interstitial flow velocities affecting solute transport was able to produce better chemistry predictions, suggesting that a multi-layered representation of snow microstructures and interstitial flow may help improve predictions. Snowmelt and ROS events, which are expected to increase in frequency as the climate warms, had a disproportionate effect on the vertical redistribution of all snow ions. Future research should focus on continuing to shed light on these heterogeneous snowpack processes of contaminant accumulation and release, as well as promote more joint efforts to attempt to simulate snow physics/hydrology and chemistry together.

CRedit authorship contribution statement

Diogo Costa: Writing – review & editing, Writing – original draft, Visualization, Validation, Supervision, Software, Resources, Project administration, Methodology, Investigation, Funding acquisition, Formal analysis, Data curation, Conceptualization. **Andrea Spolaor:** Writing – review & editing, Supervision, Methodology, Funding acquisition, Conceptualization. **Elena Barbaro:** Writing – review & editing, Supervision, Conceptualization. **Juan I. López-Moreno:** Writing – review & editing, Supervision. **John W. Pomeroy:** Writing – review & editing, Supervision, Conceptualization.

Declaration of competing interest

The authors declare the following financial interests/personal relationships which may be considered as potential competing interests: Diogo Costa reports financial support, administrative support, and writing assistance were provided by Global Water Futures. Diogo Costa and Andrea Spolaor reports financial support was provided by Research Council of Norway. Diogo Costa reports administrative support was provided by Climate Change Tower Integrated Project. If there are other authors, they declare that they have no known competing financial interests or personal relationships that could have appeared to influence the work reported in this paper.

Acknowledgements

This manuscript benefited from the support of several organizations at different phases of the research. The following organizations are acknowledged in chronological order based on their contributions: the Global Water Futures (GWF) programme, Canada; the Global Institute for Water Security (GIWS), Canada; Environment and Climate Change Canada (ECCC); the Mediterranean Institute for Agriculture, Environment and Development (MED), Portugal; the Global Changes and Sustainability Institute (CHANGE), Portugal; and the Center for Sci-Tech Research in Earth System and Energy (CREATE), Portugal.

We extend our special thanks to Mrs. Arshdeep Kaur for her initial assistance in testing the coupled models, with financial support from ECCC, Canada. Additionally, this research was supported by the Svalbard Science Forum/Research Council of Norway (grant nos. 246731/E10 and 257636/E10), and the European Union's Horizon 2020 programme (grant no. 689443, iCUPE). The authors are also grateful for the meteorological data provided by the Climate Change Tower Integrated Project (CCT-IP) of the National Research Council (<http://www.isac.cnr.it/~radioclim/CCTower/>).

Data availability

Data will be made available on request.

References

- Ardyna, M., Babin, M., Gosselin, M., Devred, E., Bélanger, S., Matsuoka, A., Tremblay, J.É., 2013. Parameterization of vertical chlorophyll α in the arctic ocean: impact of the subsurface chlorophyll maximum on regional, seasonal, and annual primary production estimates. *Biogeosciences* 10 (6), 4383–4404. <http://dx.doi.org/10.5194/bg-10-4383-2013>.
- Bales, R.C., 1991. Modeling in-pack chemical transformations. In: Davies, T.D., Tranter, M., Jones, H.G. (Eds.), *Seasonal Snowpacks*. Springer Berlin Heidelberg, Berlin, Heidelberg, pp. 139–163.
- Bales, R.C., Davis, R.E., Stanley, D.A., 1989. Ion elution through shallow homogeneous snow. *Water Resour. Res.* 25 (8), 1869–1877. <http://dx.doi.org/10.1029/WR025i008p01869>.
- Barbaro, E., Koziol, K., Björkman, M.P., Vega, C.P., Zdanowicz, C., Martma, T., Gallet, J.C., Kępski, D., Larose, C., Luks, B., Tolle, F., Schuler, T.V., Uszczyk, A., Spolaor, A., 2021. Measurement report: Spatial variations in ionic chemistry and water-stable isotopes in the snowpack on glaciers across svalbard during the 2015–2016 snow accumulation season. *Atmos. Chem. Phys.* 21 (4), 3163–3180. <http://dx.doi.org/10.5194/acp-21-3163-2021>.

- Barbaro, E., Padoan, S., Kirchgorg, T., Zangrando, R., Toscano, G., Barbante, C., Gambaro, A., 2017. Particle size distribution of inorganic and organic ions in coastal and inland Antarctic aerosol. *Environ. Sci. Pollut. Res.* 24 (3), 2724–2733. <http://dx.doi.org/10.1007/s11356-016-8042-x>.
- Bartels-Rausch, T., Jacobi, H.W., Kahan, T.F., Thomas, J.L., Thomson, E.S., Abbott, J.P.D., Ammann, M., Blackford, J.R., Bluhm, H., Boxe, C., Domine, F., Frey, M.M., Gladich, I., Guzmán, M.L., Heger, D., Huthwelker, T., Klán, P., Kuhs, W.F., Kuo, M.H., Maus, S., Moussa, S.G., McNeill, V.F., Newberg, J.T., Pettersson, J.B.C., Roeselová, M., Sodeau, J.R., 2014. A review of air–ice chemical and physical interactions (AICI): liquids, quasi-liquids, and solids in snow. *Atmos. Chem. Phys.* 14 (3), 1587–1633. <http://dx.doi.org/10.5194/acp-14-1587-2014>.
- Beldring, S., Engen-Skaugen, T., Førland, E.J., Roald, L.A., 2008. Climate change impacts on hydrological processes in Norway based on two methods for transferring regional climate model results to meteorological station sites. *Tellus A* 60 (3), 439–450. <http://dx.doi.org/10.1111/j.1600-0870.2008.00306.x>.
- Beniston, M., Stoffel, M., 2016. Rain-on-snow events, floods and climate change in the Alps: Events may increase with warming up to 4 °C and decrease thereafter. *Sci. Total Environ.* 571, 228–236. <http://dx.doi.org/10.1016/J.SCITOTENV.2016.07.146>.
- Boike, J., Juszak, I., Lange, S., Chadburn, S., Burke, E., Overduin, P.P., Roth, K., Ippisch, O., Bornemann, N., Stern, L., Gouttevin, I., Hauber, E., Westermann, S., 2018. A 20-year record (1998–2017) of permafrost, active layer and meteorological conditions at a high Arctic permafrost research site (Bayelva, Spitsbergen). *Earth Syst. Sci. Data* 10 (1), 355–390. <http://dx.doi.org/10.5194/essd-10-355-2018>.
- Brimblecombe, P., Tranter, M., Abrahams, P.W., Blackwood, I., Davies, T.D., Vincent, C.E., 1985. Relocation and preferential elution of acidic solute through the snowpack of a small, remote, high-altitude scottish catchment. *Ann. Glaciol.* 7, 141–147. <http://dx.doi.org/10.3189/S0260305500006066>.
- Brimblecombe, P., Tranter, M., Tsiouris, S., Davies, T.D., Vincent, C.E., 1986. The chemical evolution of snow and meltwater. *IAHS Publ.* 155, 283–295.
- Charbeneau, R., Daniel, D., Maidment, D., 1992. Contaminant transport in unsaturated flow. In: *Handbook of Hydrology*. McGraw-Hill Inc, New York, (Chap. 15).
- Costa, D., A Sextstone, G., W Pomeroy, J., H Campbell, D., W Clow, D., Mast, A., 2020. Preferential elution of ionic solutes in melting snowpacks: Improving process understanding through field observations and modeling in the Rocky Mountains. *Sci. Total Environ.* 710, 136273. <http://dx.doi.org/10.1016/j.scitotenv.2019.136273>.
- Costa, D., Liu, J., Roste, J., Elliott, J., 2019. Temporal dynamics of snowmelt nutrient release from snow–plant residue mixtures: An experimental analysis and mathematical model development. *J. Environ. Qual.* 48 (4), 869–879. <http://dx.doi.org/10.2134/jeq2018.12.0440>.
- Costa, D., Pomeroy, J.W., 2019. Preferential meltwater flowpaths as a driver of preferential elution of chemicals from melting snowpacks. *Sci. Total Environ.* 662, 110–120. <http://dx.doi.org/10.1016/J.SCITOTENV.2019.01.091>.
- Costa, D., Pomeroy, J., Wheeler, H., 2018. A numerical model for the simulation of snowpack solute dynamics to capture runoff ionic pulses during snowmelt: The PULSE model. *Adv. Water Resour.* 122, 37–48. <http://dx.doi.org/10.1016/j.advwatres.2018.09.008>.
- Costa, D., Roste, J., Pomeroy, J., Baulch, H., Elliott, J., Wheeler, H., Westbrook, C., 2017. A modelling framework to simulate field-scale nitrate response and transport during snowmelt: The WINTRA model. *Hydrol. Process.* 31 (24), 4250–4268.
- Cragin, J., Hewitt, A., Colbeck, S., 1993. Elution of Ions from Melting Snow: Chromatographic Versus Metamorphic Mechanisms. CRREL Report 93–8, US Army Corps of Engineers, Cold Regions Research & Engineering Laboratory, URL: <https://apps.dtic.mil/sti/tr/pdf/ADA270430.pdf>.
- Dagsson-Waldhauserova, P., Meinander, O., 2019. Editorial: Atmosphere–Cryosphere interaction in the arctic, at high latitudes and mountains with focus on transport, deposition, and effects of dust, black carbon, and other aerosols. *Front. Earth Sci.* 7, <http://dx.doi.org/10.3389/feart.2019.00337>.
- Davies, T.D., Brimblecombe, P., Tranter, M., Tsiouris, S., Vincent, C.E., Abrahams, P., Blackwood, I.L., 1987. The removal of soluble ions from melting snowpacks. In: Jones, H.G., Orville-Thomas, W.J. (Eds.), *Seasonal Snowcovers: Physics, Chemistry, Hydrology*. In: NATO ASI Series (Series C: Mathematical and Physical Sciences), Springer Netherlands, Dordrecht, pp. 337–392. http://dx.doi.org/10.1007/978-94-009-3947-9_20.
- Davis, R.E., Petersen, C.E., Bales, R.C., 1995. Ion flux through a shallow snowpack: effects of initial conditions and melt sequences. In: Tonnessen, K., Williams, M., Tranter, M. (Eds.), *Biogeochemistry of Seasonally Snow-Covered Catchments*. (Proceedings of a Boulder Symposium, July 1995). IAHS Publ. no. 228, pp. 115–128.
- Gondwe, M., Krol, M., Gieskes, W., Klaassen, W., de Baar, H., 2003. The contribution of ocean-leaving DMS to the global atmospheric burdens of DMS, MSA, SO₂, and NSS SO₄-. *Glob. Biogeochem. Cycles* 17 (2), <http://dx.doi.org/10.1029/2002GB001937>.
- Hansen, B.B., Isaksen, K., Benestad, R.E., Kohler, J., Pedersen, Å.Ø., Loe, L.E., Coulson, S.J., Larsen, J.O., Varpe, Ø., 2014. Warmer and wetter winters: characteristics and implications of an extreme weather event in the High Arctic. *Environ. Res. Lett.* 9 (11), 114021. <http://dx.doi.org/10.1088/1748-9326/9/11/114021>.
- Harrington, R., Bales, R.C., 1998. Modeling ionic solute transport in melting snow. *Water Resour. Res.* 34 (7), 1727–1736. <http://dx.doi.org/10.1029/98WR00557>.
- Harrington, R., Bales, R.C., Wagon, P., 1996. Variability of meltwater and solute fluxes from homogeneous melting snow at the laboratory scale. *Hydrol. Process.* 10 (7), 945–953. [http://dx.doi.org/10.1002/\(SICI\)1099-1085\(199607\)10:7<945:AIID-HYP349>3.0.CO;2-S](http://dx.doi.org/10.1002/(SICI)1099-1085(199607)10:7<945:AIID-HYP349>3.0.CO;2-S).
- Hewitt, A.D., Cragin, J.H., Colbeck, S.C., 1991. Effects of crystal metamorphism on the elution of chemical species from snow. In: *Proceedings of the 48th Annual Eastern Snow Conference*. Guelph, Ontario, Canada, pp. 1–10.
- Hibberd, S., 1984. A model for pollutant concentrations during snow-melt. *J. Glaciol.* 30 (104), 58–65.
- Hirashima, H., Yamaguchi, S., Sato, A., Lehning, M., 2010. Numerical modeling of liquid water movement through layered snow based on new measurements of the water retention curve. *Cold Reg. Sci. & Technol.* 64 (2), 94–103. <http://dx.doi.org/10.1016/j.coldregions.2010.09.003>.
- Hodson, A., Anesio, A.M., Tranter, M., Fountain, A., Osborn, M., Priscu, J., Laybourn-Parry, J., Sattler, B., 2008. Glacial ecosystems. *Ecol. Monograph.* 78 (1), 41–67. <http://dx.doi.org/10.1890/07-0187.1>.
- Isaksen, K., Nordli, Ø., Førland, E.J., Łupikasza, E., Eastwood, S., Niedźwiedz, T., 2016. Recent warming on Spitsbergen—Influence of atmospheric circulation and sea ice cover. *J. Geophys. Res.: Atmos.* 121 (20), 11,911–913,931. <http://dx.doi.org/10.1002/2016JD025606>.
- Johannessen, M., Dale, T., Gjessing, E., Henriksen, A., Wright, R., 1976. Acid precipitation in Norway: the regional distribution of contaminants in snow and the concentration processes during snowmelt. In: *IAHS Publ.*, vol. 118, pp. 116–120.
- Johannessen, M., Henriksen, A., 1978. Chemistry of snow meltwater: Changes in concentration during melting. *Water Resour. Res.* 14 (4), 615–619. <http://dx.doi.org/10.1029/WR014i004p00615>.
- Jones, H.G., Davies, T.D., Pomeroy, J.W., Marsh, P., Tranter, M., 1993. Snow-atmosphere interactions in arctic snowpacks. In: *Proceedings of the Eastern Snow Conference*, vol. 61, Colorado State University, p. 255.
- Kane, D.L., Yang, D., 2004. Northern research basins water balance. In: *Northern Research Basins Water Balance*. In: IAHS Publ., vol. 290, p. vii+90.
- Keenan, E., Wever, N., Dattler, M., Lenaerts, J.T.M., Medley, B., Kuipers Munneke, P., Reijmer, C., 2021. Physics-based SNOWPACK model improves representation of near-surface Antarctic snow and firm density. *Cryosphere* 15 (2), 1065–1085. <http://dx.doi.org/10.5194/tc-15-1065-2021>.
- Kühnel, R., Roberts, T.J., Björkman, M.P., Isaksson, E., Aas, W., Holmén, K., Ström, J., 2011. 20-Year climatology of and wet deposition at Ny-Ålesund, Svalbard. *Adv. Meteorol.* 2011 (2011), <http://dx.doi.org/10.1155/2011/406508>.
- Lapalme, C.M., Spence, C., Costa, D., Bonsal, B.R., Musetta-Lambert, J., Fazli, Y., 2023. Towards the incorporation of hydrogeochemistry into the modelling of permafrost environments: a review of recent recommendations, considerations, and literature. *Arct. Sci.* 9 (4), 750–768. <http://dx.doi.org/10.1139/as-2022-0038>.
- Larose, C., Dommergue, A., Vogel, T.M., 2013a. The dynamic arctic snow pack: an unexplored environment for microbial diversity and activity. *Biology* 2 (1), 317–330. <http://dx.doi.org/10.3390/biology2010317>.
- Larose, C., Prestat, E., Cecillon, S., Berger, S., Malandain, C., Lyon, D., Ferrari, C., Schneider, D., Dommergue, A., Vogel, T.M., 2013b. Interactions between snow chemistry, mercury inputs and microbial population dynamics in an arctic snowpack. *PLoS One* 8 (11), e79972. <http://dx.doi.org/10.1371/journal.pone.0079972>, (Research Article).
- Lehning, M., Bartel, P., Brown, B., Fierz, C., Satyawali, P., 2002. A physical SNOWPACK model for the Swiss avalanche warning: Part II. Snow microstructure. *Cold Reg. Sci. & Technol.* 35 (3), 147–167. [http://dx.doi.org/10.1016/S0165-232X\(02\)00073-3](http://dx.doi.org/10.1016/S0165-232X(02)00073-3).
- Leroux, N.R., Pomeroy, J.W., 2017. Modelling capillary hysteresis effects on preferential flow through melting and cold layered snowpacks. *Adv. Water Resour.* 107, 250–264. <http://dx.doi.org/10.1016/j.advwatres.2017.06.024>.
- Leroux, N.R., Pomeroy, J.W., 2019. Simulation of capillary pressure overshoot in snow combining trapping of the wetting phase with a nonequilibrium Richards equation model. *Water Resour. Res.* 55 (1), 236–248. <http://dx.doi.org/10.1029/2018WR022969>.
- Lilbæk, G., Pomeroy, J.W., 2008. Ion enrichment of snowmelt runoff water caused by basal ice formation. *Hydrol. Process.* 22 (15), 2758–2766. <http://dx.doi.org/10.1002/hyp.7028>.
- Lilbæk, G., Pomeroy, J.W., 2010. Laboratory evidence for enhanced infiltration of ion load during snowmelt. *Hydrol. Earth Syst. Sci.* 14 (7), 1365–1374. <http://dx.doi.org/10.5194/hess-14-1365-2010>.
- López-Moreno, J.I., Boike, J., Sanchez-Lorenzo, A., Pomeroy, J.W., 2016. Impact of climate warming on snow processes in Ny-Ålesund, a polar maritime site at Svalbard. *Glob. Planet. Change* 146 (C), 10–21. <http://dx.doi.org/10.1016/j.gloplacha.2016.09.006>.
- López-Moreno, J.I., Goyette, S., Beniston, M., 2009. Impact of climate change on snowpack in the Pyrenees: Horizontal spatial variability and vertical gradients. *J. Hydrol.* 374 (3), 384–396. <http://dx.doi.org/10.1016/j.jhydrol.2009.06.049>.
- Marsh, P., Pomeroy, J.W., 1999. Spatial and temporal variations in snowmelt runoff chemistry, Northwest Territories, Canada. *Water Resour. Res.* 35 (5), 1559–1567. <http://dx.doi.org/10.1029/1998WR900109>.

- Maturilli, M., Herber, A., König-Langlo, G., 2013. Climatology and time series of surface meteorology in Ny-Ålesund, Svalbard. *Earth Syst. Sci. Data* 5, 155–163. <http://dx.doi.org/10.5194/essd-5-155-2013>.
- Morán-Tejeda, E., López-Moreno, J., Stoffel, M., Beniston, M., 2016. Rain-on-snow events in Switzerland: recent observations and projections for the 21st century. *Clim. Res.* 71 (2), 111–125. <http://dx.doi.org/10.3354/cr01435>.
- Nawrot, A.P., Migala, K., Luks, B., Pakszys, P., Głowacki, P., 2016. Chemistry of snow cover and acidic snowfall during a season with a high level of air pollution on the Hans Glacier, Spitsbergen. *Polar Sci.* 10 (3), 249–261. <http://dx.doi.org/10.1016/j.polar.2016.06.003>.
- Nordli, Ø., Przybylak, R., Ogilvie, A.E.J., Isaksen, K., 2014. Long-term temperature trends and variability on Spitsbergen: the extended Svalbard Airport temperature series, 1898–2012. *Polar Res.* 33 (0 SE - Research/review articles), <http://dx.doi.org/10.3402/polar.v33.21349>.
- Nowak, A., Hodson, A., 2013. Hydrological response of a High-Arctic catchment to changing climate over the past 35 years: a case study of Bayelva watershed, Svalbard. *Polar Res.* 32 (1), <http://dx.doi.org/10.3402/polar.v32i0.19691>.
- Ouellet, F., Langlois, A., Blukacz-Richards, E.A., Johnson, C.A., Royer, A., Neave, E., Larter, N.C., 2017. Spatialization of the SNOWPACK snow model for the Canadian Arctic to assess Peary caribou winter grazing conditions. *Phys. Geogr.* 38 (2), 143–158. <http://dx.doi.org/10.1080/02723646.2016.1274200>.
- Pollock, M.D., O'Donnell, G., Quinn, P., Dutton, M., Black, A., Wilkinson, M.E., Colli, M., Stagnaro, M., Lanza, L.G., Lewis, E., Kilsby, C.G., O'Connell, P.E., 2018. Quantifying and mitigating wind-induced undercatch in rainfall measurements. *Water Resour. Res.* 54 (6), 3863–3875. <http://dx.doi.org/10.1029/2017WR022421>.
- Pomeroy, J.W., Brown, T., Fang, X., Shook, K.R., Pradhananga, D., Armstrong, R., Harder, P., Marsh, C., Costa, D., Krogh, S.A., Aubry-Wake, C., Annand, H., Lawford, P., He, Z., Kompanizare, M., Lopez Moreno, J.I., 2022. The cold regions hydrological modelling platform for hydrological diagnosis and prediction based on process understanding. *J. Hydrol.* 615, 128711. <http://dx.doi.org/10.1016/j.jhydrol.2022.128711>.
- Pomeroy, J.W., Davies, T.D., Tranter, M., 1991. The impact of blowing snow on snow chemistry. In: *Seasonal Snowpacks: Processes of Compositional Change*. Springer, Heidelberg, pp. 71–113. http://dx.doi.org/10.1007/978-3-642-75112-7_4.
- Pomeroy, J.W., Gray, D.M., 1990. Saltation of snow. *Water Resour. Res.* 26 (7), 1583–1594. <http://dx.doi.org/10.1029/WR026i007p01583>.
- Pomeroy, J.W., Gray, D.M., Brown, T., Hedstrom, N.R., Quinton, W.L., Granger, R.J., Carey, S.K., 2007. The cold regions hydrological model: A platform for basing process representation and model structure on physical evidence. In: Martz, L., Buttle, J. (Eds.), *Hydrol. Process.* 21 (19), 2650–2667. <http://dx.doi.org/10.1002/hyp.6787>.
- Pomeroy, J.W., Li, L., 2000. Prairie and arctic areal snow cover mass balance using a blowing snow model. *J. Geophys. Res.* 105 (D21), 26619–26634. <http://dx.doi.org/10.1029/2000JD900149>.
- Pomeroy, J.W., Marsh, P., Lesack, L., 1993. Relocation of major ions in snow along the Tundra-Taiga ecotone. *Hydrol. Res.* 24 (2–3), 151–168.
- Rinke, A., Maturilli, M., Graham, R.M., Matthes, H., Handorf, D., Cohen, L., Hudson, S.R., Moore, J.C., 2017. Extreme cyclone events in the Arctic: Wintertime variability and trends. *Environ. Res. Lett.* 12 (9), 094006. <http://dx.doi.org/10.1088/1748-9326/aa7def>.
- Salzano, R., Cerrato, R., Scoto, F., Spolaor, A., Valentini, E., Salvatore, M., Esposito, G., Sapio, S., Taramelli, A., Salvatori, R., 2023. Detection of winter heat wave impact on surface runoff in a periglacial environment (Ny-Ålesund, Svalbard). *Remote Sens.* 15 (18), <http://dx.doi.org/10.3390/rs15184435>.
- Schmucki, E., Marty, C., Fierz, C., Lehning, M., 2014. Evaluation of modelled snow depth and snow water equivalent at three contrasting sites in Switzerland using SNOWPACK simulations driven by different meteorological data input. *Cold Reg. Sci. & Technol.* 99, 27–37. <http://dx.doi.org/10.1016/j.coldregions.2013.12.004>.
- Smith, C.D., Ross, A., Kochendorfer, J., Earle, M.E., Wolff, M., Buisán, S., Roulet, Y.A., Laine, T., 2020. Evaluation of the WMO Solid Precipitation Intercomparison Experiment (SPICE) transfer functions for adjusting the wind bias in solid precipitation measurements. *Hydrol. Earth Syst. Sci.* 24 (8), 4025–4043. <http://dx.doi.org/10.5194/hess-24-4025-2020>.
- Spolaor, A., Barbaro, E., Christille, J.M., Kirchgorg, T., Giardi, F., Cappelletti, D., Turetta, C., Bernagozzi, A., Björkman, M.P., Bertolini, E., Barbante, C., 2016. Evolution of the svalbard annual snow layer during the melting phase. *Rend. Lincei - Sci. Fis. Natur.* 27 (1), 147–154.
- Spolaor, A., Luks, B., Gallet, J.-C., Salzano, R., Pohjola, V.A., Costa, D., 2023. Editorial: Pan-Arctic snow research. *Front. Earth Sci.* 11, <http://dx.doi.org/10.3389/feart.2023.1266810>.
- Spolaor, A., Varin, C., Pedeli, X., Christille, J.M., Kirchgorg, T., Giardi, F., Cappelletti, D., Turetta, C., Cairns, W.R.L., Gambaro, A., Bernagozzi, A., Gallet, J.C., Björkman, M.P., Barbaro, E., 2021. Source, timing and dynamics of ionic species mobility in the Svalbard annual snowpack. *Sci. Total Environ.* 751, 141640. <http://dx.doi.org/10.1016/j.scitotenv.2020.141640>.
- Stein, J., Jones, H., Roberge, J., Sochanska, W., 1986. The prediction of both runoff quality and quantity by the use of an integrated snowmelt model. *IAHS-AISH Publ.* (155), 347–358.
- Vershegy, D.L., 1991. Class—A Canadian land surface scheme for GCMS. I. Soil model. *Int. J. Climatol.* 11 (2), 111–133. <http://dx.doi.org/10.1002/joc.3370110202>.
- Virkkunen, K., Moore, J.C., Isaksson, E., Pohjola, V., Perämäki, P., Grinsted, A., Kekonen, T., 2007. Warm summers and ion concentrations in snow: comparison of present day with Medieval Warm Epoch from snow pits and an ice core from Lomonosovfonna, Svalbard. 2017/09/08 *J. Glaciol.* 53 (183), 623–634. <http://dx.doi.org/10.3189/002214307784409388>.
- Yuan, L., Sun, L., Long, N., Xie, Z., Wang, Y., Liu, X., 2010. Seabirds colonized Ny-Ålesund, Svalbard, Arctic ~9400 years ago. *Polar Biol.* 33 (5), 683–691. <http://dx.doi.org/10.1007/s00300-009-0745-8>.